Colloid Polym Sci (2007) 285:389–396
DOI 10.1007/s00396-006-1556-x

ORIGINAL CONTRIBUTION

Reactivity of some sulphur- and non-sulphur-containing amino acids towards water soluble colloidal MnO_2. A kinetic study

Syed Misbah Zahoor Andrabi · Zaheer Khan

Received: 30 March 2006 / Accepted: 30 June 2006 / Published online: 3 November 2006

Abstract Kinetic data for the oxidation of glutathione (reduced, GSH), cysteine, glycine and glutamic acid by colloidal manganese dioxide, $(MnO_2)_n$ are reported. Colloidal MnO_2, oxidized glutathione to disulphide (glutathione, oxidized), was reduced to manganese (II). Glycine and glutamic acid (structural units of glutathione) are not oxidized by colloidal MnO_2, but the other structural unit, cysteine, is also oxidized by the same oxidant under similar experimental conditions. This is interpreted in terms of the rate-determining colloidal MnO_2-S bonded intermediate. The reactivity of GSH towards colloidal MnO_2 is very much higher than cysteine. Kinetics of oxidation of GSH and cysteine by colloidal MnO_2 were performed spectrophotometrically as a function of [GSH], [cysteine], colloidal $[(MnO_2)_n]$, $[HClO_4]$, temperature and trapping agents sodium fluoride and manganese (II) (reduction product of colloidal MnO_2). The purpose of this work was to study the role of $–NH_2$, –COOH, –SH groups present in the carbon chain of the above amino acids. It was found that the reactivity of –SH group is higher than $–NH_2$ and –COOH groups. The mechanisms, involving a colloidal MnO_2 complex with GSH and cysteine, are proposed. The complexes decompose in a rate-determining step, leading to the formation of free radical and manganese (III), which is also an intermediate. The dimerization of radicals takes place in a subsequent fast step to yield the products.

Keywords Oxidation · Glutathione · Cysteine · Colloidal MnO_2 · Kinetics · Glutamic acid

S. M. Z. Andrabi · Z. Khan (✉)
Department of Chemistry, Jamia Millia Islamia, Jamia Nagar, New Delhi 110025, India
e-mail: drkhanchem@yahoo.co.in

Introduction

Glutathione (γ-glutamylcysteinylglycine, GSH) is a biologically important reductant, which exists in mammalian cells, making it the most prevalent intracellular thiol. It is well documented that glutathione (GSH) and L-cysteine have rich redox chemistry as reductants in aqueous solution [1–5]. GSH is a bioactive ligand and an essential tripeptide found in most living cells. Amino acids serve important functions in biological systems and are employed in biochemical, microbiological and nutrition investigations. The reaction of GSH with different transition metal ion oxidants has been investigated [1–5] on several occasions. GSH has eight coordination centers: two-COOH oxygens, one amine nitrogen, two peptide nitrogens, two peptide oxygens and one thiol group. Sulphur has been established as the most susceptible to attack by the oxidant [6–8].

The evidence for the existence of manganese (IV) in the colloidal state has been obtained by several investigators [9–16]. A perfectly transparent and water soluble colloidal manganese (IV) species, $(MnO_2)_n$, was obtained by Perez-Benito et al. [17, 18] by the oxidation of sodium-thiosulphate with potassium permanganate in neutral aqueous solution. The transparent sols of manganese dioxide are of importance due to their involvement as active autocatalysts in many permanganate reactions [19, 20]. The oxidative degradation of organic acids [21–24], carbohydrates [25, 26] and thiourea [27] by water soluble colloidal MnO_2 has received some attention.

Afonso and his co-workers [5] have carried out the reaction of GSH and cysteine with colloidal MnO_2 using stopped-flow system coupled to a UV-visible diode array spectrophotometer. Here, the reaction is completed in less than 1 min. They have also reported the higher reactivity of cysteine in comparison to glutathione. Considering the

significance of GSH as a master antioxidant and intracellular sulfhydryl buffer, it was thought that the knowledge of the kinetics of all the constituents of this tripeptide (cysteine, glycine and glutamic acid) in a different reaction system for a longer time period could be interesting to permit reasonable comparison of the kinetic data. This paper deals with the kinetics and mechanism oxidation of glutathione, cysteine, glycine and glutamic acid by colloidal MnO_2.

Experimental

Materials

Glutathione (reduced) (LOBA), L-cysteine, (Merck, India), glycine (Merck, India), glutamic acid (Sisco, India) were used as received. A standard solution of perchloric acid (Fisher, 70% reagent) was prepared and analyzed by titration against sodiumtetraborate. The solvent water was purified by deionization followed by double distillation. Water-soluble colloidal MnO_2 was prepared by the reported methods of Perez-Benito et al. [17, 18]. All the reagents (potassium permanganate, sodium thiosulphate, sodium fluoride, manganese (II) chloride) used were supplied by Merck, India and were of commercially available purity.

Kinetic measurements

The kinetics of the redox reactions was carried out in a three-necked reaction flask fitted with a double-walled condenser (to check evaporation). The reaction was initiated by adding to the reaction mixture thermally equilibrated at 30 °C (±0.1 °C) a requisite amount of reductant pre-equilibrated at the same temperature. The progress of the reaction was monitored spectrophotometrically by measuring the absorbance of the remaining colloidal MnO_2 at 375 nm at regular intervals on a spectronic 21-D spectrophotometer. All the reactions were usually followed up to not less than 80% completion. Other details of the kinetic experiments were the same as described elsewhere [22–25].

Product analysis

Glutathione (oxidized) and cystine, as the oxidation products of GSH and cysteine by colloidal MnO_2, were characterized on the basis of disulphide linkage [28, 29]. For the oxidation products of GSH and cysteine, qualitative analysis of the oxidized reaction mixture was performed. After ensuring completion of the reaction, the oxidized reaction mixture was treated with 200 cm^3 of ethanol followed by 60 cm^3 of concentrated HCl solution. It resulted in the formation of white crystals of dithiobis (formadinium). The compound was identified by the reported method [29]. These results are in good agreement with those found for other similar reactions (thiols are oxidized by most oxidants to the corresponding disulphide) [30–32].

Results and discussion

Oxidation of glutathione

Under the pseudo first-order conditions (GSH>colloidal MnO_2), the dark brown reaction mixture containing colloidal MnO_2 (1.0×10^{-5} mol dm^{-3}) became colorless immediately in the presence of small amount of GSH ($\geq1.0\times10^{-4}$ mol dm^{-3}). Therefore, the choice of the best conditions for the kinetic experiments was a crucial problem that we addressed first. To evaluate the rate constants, kinetic experiments were performed under second-order conditions. It has been observed [26] that minimum amounts of different electrolytes are necessary for the precipitation of MnO_2. The reason for this is that colloidal particles take up ions carrying an opposite charge to that present on themselves. Therefore, it is to be mentioned that the ionic strength of the reaction mixture could not be maintained constant. The rate of disappearance of colloidal MnO_2 is shown in Fig. 1 as absorbance–time profile. On mixing glutathione and colloidal MnO_2 in neutral to acidic pH, there is an initially fast reaction. After

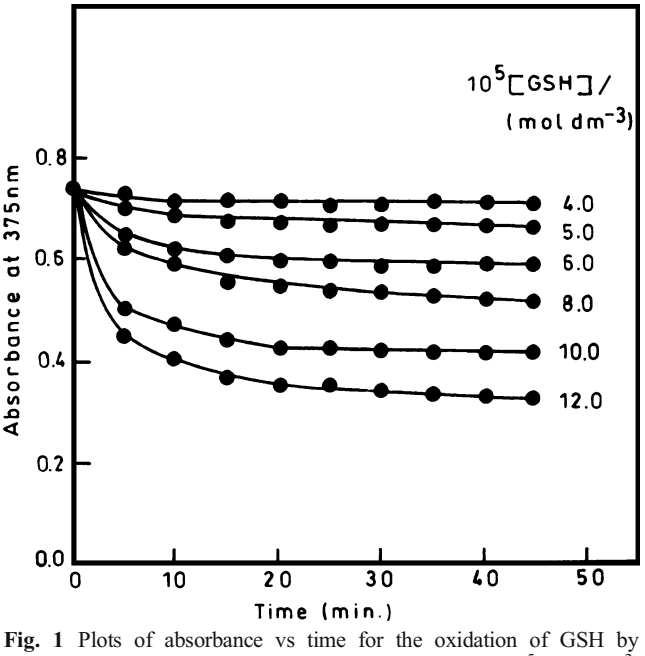

Fig. 1 Plots of absorbance vs time for the oxidation of GSH by colloidal MnO_2. Reaction conditions: $[(MnO_2)_n]=8.0\times10^{-5}$ mol dm^{-3}; temperature=30 °C

this, the remaining colloidal MnO_2 is consumed much more slowly.

The stoichiometry of the reaction was determined by carrying out the reactions with an excess of MnO_2 over GSH. The excess of colloidal MnO_2 was determined spectrophotometrically. Under our experimental conditions, 1 mol of colloidal MnO_2 consumed 2 mol of GSH in 20 min at 25 °C. Therefore, the reaction may be represented stoichiometrically by the equation:

$$\begin{aligned} &2\ \text{Glutathione (reduced)} \\ &+\ MnO_2 \longrightarrow \text{Glutathione (oxidized)} \\ &+\ Mn^{2+} + 2OH^- \end{aligned} \quad (1)$$

Thus, we have used Eqs. 2 and 3 to evaluate the second-order rate constant (k_{obs}, $mol^{-1}\ dm^3\ s^{-1}$)

$$k_{obs} = \frac{4.606}{t(2a-b)} log \frac{b(2a-x)}{2a(b-x)} \quad 2a > b \quad (2)$$

$$k_{obs} = \frac{4.606}{t(b-2a)} log \frac{2a(b-x)}{b(2a-x)} \quad b > 2a \quad (3)$$

The values of k_{obs} were calculated from slopes of $\log[b(2a-x)/2a(b-x)]$ or $\log[2a(b-x)/b(2a-x)]$ vs time.

It was observed that at constant [GSH], the values of second-order rate constant decrease with $[(MnO_2)_n]$ (Table 1), *vide infra.* The reaction rate increased with increase in [GSH] and the plot of rate constants vs [GSH] is nonlinear passing through the origin, which shows the characteristic of second-order reaction. To verify the role of hydrogen ion, some kinetic runs were also performed in the presence of $HClO_4$. The rate constants increased markedly with increase in $[H^+]$ (Table 1). The plot of rate constant vs $[HClO_4]$ was a straight line with positive intercept on the *y*-axis (Fig. not shown). The effect of $[HClO_4]$ shows, conclusively, that oxidation of GSH proceeds through the adsorption of H^+ and GSH on the surface of colloidal MnO_2.

Table 1 Observed rate constants for the reaction of colloidal MnO_2 and GSH in absence and presence of $HClO_4$

$10^5[MnO_2]$ (mol dm^{-3})	10^5[GSH (mol dm^{-3})	$10^4[HClO_4]$ (mol dm^{-3})	Temp. (°C)	k_{obs} (mol^{-1} dm^3 s^{-1})
5.0	6.0	0.0	30	5.0
6.0				3.2
7.0				2.8
8.0				1.7
9.0				1.3
8.0	4.0	0.0	30	0.8
	5.0			1.1
	6.0			1.7
	8.0			2.3
	10.0			3.0
	12.0			4.1
8.0	6.0	0.0	30	1.7
			40	2.1
			50	2.5
8.0	6.0	0.0	30	1.7
		0.93		5.3
		1.86		8.8
		2.79		11.2
		3.72		14.4

The formation of an intermediate between GSH and colloidal MnO_2 was confirmed from initial absorbance increase at 375 nm at lower [GSH]. The preliminary observations indicated that the absorbance of colloidal MnO_2 (8.0×10^{-5} mol dm^{-3}) changes with GSH ($\leq 2.0\times10^{-5}$ mol dm^{-3}). The initial rapid reaction may be represented as [29, 33]:

$$(MnO_2)_n + GSH \underset{}{\overset{K_{ad1}}{\rightleftharpoons}} (MnO_2)_n\text{—}GSH \quad (4)$$

the value of K_{ad1} was determined using Eq. 5

$$\frac{[(MnO_2)_n][GSH]}{\triangle A} = \frac{[GSH]}{\triangle \varepsilon 1} + \frac{1}{K_{ad1}\triangle \varepsilon 1} \quad (5)$$

where ΔA=the difference in the absorbance between the complex and colloidal MnO_2 at 375 nm where both uncomplexed and complexed forms of colloidal MnO_2 absorb, $\Delta\varepsilon$=difference in the absorption coefficients and l=the path length (1 cm). The data in Fig. 2 represent some

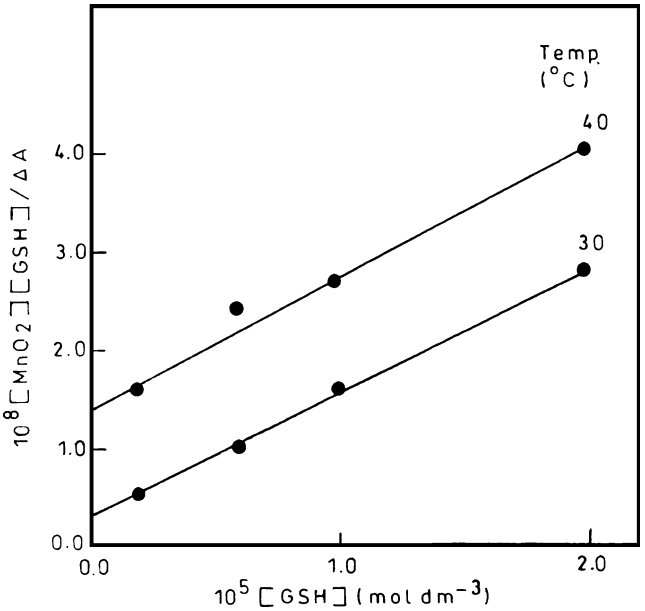

Fig. 2 Plots of left-hand-side of Eq. 5 vs [GSH]. Reaction conditions: $[(MnO_2)_n]=8.0\times10^{-5}$ mol dm^{-3}; temperature=30 °C

Table 2 Values of initial complex formation constants (K_{ad1}) using Eq. 5 and activation parameters for the oxidation of GSH and cysteine by colloidal MnO_2

Parameters	GSH[a]	Cysteine[b]
$10^{-4}K_{ad1}$ (mol^{-1} dm^3)	34.6 (9.2)	
$\Delta\varepsilon$ (mol^{-1} dm^3 cm^{-1})	962 (769)	
E_a (kJ mol^{-1})	16	20
$\Delta H^{\#}$ (kJ mol^{-1})	14	17
$\Delta S^{\#}$ (J $K^{-1}mol^{-1}$)	−268	−241

[a] $[GSH] \leq 0.2\times10^{-5}$ mol dm^{-3}, colloidal $[(MnO_2)_n]=8.0\times10^{-5}$ mol dm^{-3}; temperature=30 °C. The value of K_{ad1} and $\Delta\varepsilon$ at 40 °C are given in parenthesis.

[b] [cysteine]=3.0×10^{-4} mol dm^{-3}, colloidal $[(MnO_2)_n]=3.0\times10^{-5}$ mol dm^{-3}; temperature=30 °C

of the initial absorbance changes presented in the form of Eq. 5 from which both the adsorption constants and the absorption coefficients may be derived. These values are summarized in Table 2. Increase in temperature also increases the rate of oxidation of GSH (Table 1). From the Arrhenius (log k vs $1/T$) plot, Fig. 5, the energy of activation (E_a), enthalpy of activation ($\Delta H^{\#}$) and entropy of activation ($\Delta S^{\#}$) were also calculated. The activation parameters are summarized in Table 2.

On the basis of the above results, the steps of the redox reaction can be written as shown in Scheme 1:

The role of hydrogen ion can be explained by considering reactions 7 and 8 of Scheme 1. As the $[H^+]$ increases, the probability of H^+-$(MnO_2)_n$-GSH formation increases which, in turn, increases the reaction rate.

Consequently, the rate may be explained by the simple rate—Eq. 6

$$\frac{-d\left[(MnO_2)_n\right]}{dt} = \frac{\left(K_{ad1}k_1 + K_{ad1}'k_1'K_p\left[H^+\right]^2\right)\left[(MnO_2)_n\right][GSH]}{\left(1+K_p\left[H^+\right]\right)} \quad (6)$$

Oxidation of L-cysteine

A series of experiments were performed in aqueous medium with cysteine concentration varying within the range from 3.0×10^{-4} to 7.0×10^{-4} mol dm^{-3} at constant colloidal $MnO_2=3.0\times10^{-5}$ mol dm^{-3} at 30 °C. In all cases, [cysteine] was in large excess (≥tenfold) to work under *pseudo*-first-order conditions. The absorbance decay of colloidal MnO_2 solution with time in the presence of cysteine is shown graphically in Fig. 3. The reaction–time curves were all sigmoid in nature throughout the entire range and the initial rates were, therefore, determined from the measurements of the slopes of the initial tangents to the reaction–time curves.

Scheme 1 The steps of the redox reaction

H^+ - independent

$$(MnO_2)_n + GSH \underset{}{\overset{K_{ad1}}{\rightleftharpoons}} (MnO_2)_n\text{—}GSH \quad (1)$$

$$(MnO_2)_n\text{—}GSH \xrightarrow{k_1} (MnO_2)_{n-1}\text{—}MnO_2H + Radical \quad (2)$$

$$(MnO_2)_{n-1}\text{–}MnO_2H + H^+ \xrightarrow{fast} Mn^{3+} + (MnO_2)_{n-1} + 2OH^- \quad (3)$$

$$Mn^{3+} + GSH \xrightarrow{fast} Mn^{2+} + Radical \quad (4)$$

$$2\ Radicals \xrightarrow[dimerization]{fast} \underset{(P)}{GSH\ (oxidized)} \quad (5)$$

H^+ – dependent

$$(MnO_2)_n + H^+ \overset{K_p}{\rightleftharpoons} (MnO_2)_n\text{—}H^+ \quad (6)$$

$$\underset{(A)}{GSH} + H^+ \overset{K_a}{\rightleftharpoons} \underset{(HA)}{GSH_2} \quad (7)$$

$$(MnO_2)_n\text{—}H^+ + HA \overset{K_{ad1}'}{\rightleftharpoons} \underset{\mathbf{(C1)}}{GSH_2\text{—}(MnO_2)_n\text{—}H^+} \quad (8)$$

$$(C1) \xrightarrow{k_1'} (MnO_2)_{n-1}\text{—}MnO_2H + Radical \quad (9)$$

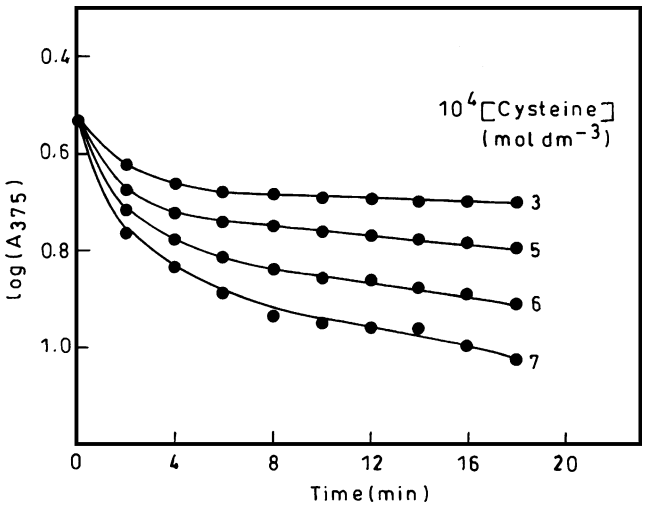

Fig. 3 Plots of log (absorbance) vs time for the oxidation of cysteine by colloidal MnO_2. Reaction conditions: $[(MnO_2)_n]=3.0\times10^{-5}$ mol dm^{-3}: temperature=30 °C

The dependence of the observed first-order rate constant on [cysteine] was also investigated. Figure 4 shows the plots of k_{obs} vs [cysteine] and $[HClO_4]$. The plot, k_{obs}−cysteine, is a straight line passing through the origin indicating first-order dependence on [cysteine], whereas, k_{obs}−$HClO_4$ plot is nonlinear and exhibits meaningful intercept on the *y*-axis suggesting acid-independent and acid-dependent paths being involved in the reduction of

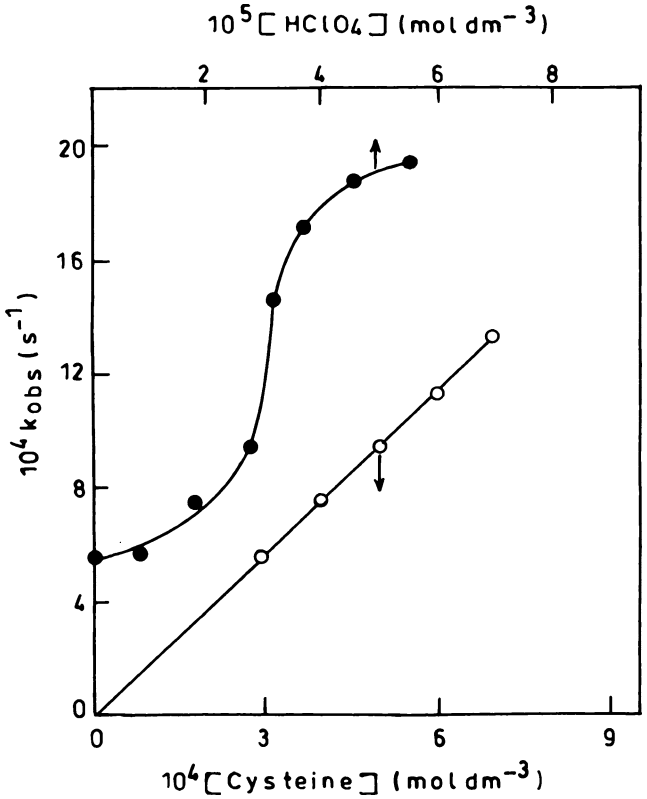

Fig. 4 Plots of k_{obs} vs [cysteine] and $[HClO_4]$. Reaction conditions: $[(MnO_2)_n]=3.0\times10^{-5}$ mol dm^{-3}; temperature=30 °C

Table 3 Observed rate constants for the reaction of colloidal MnO_2 and cysteine in absence and presence of $HClO_4$

$10^5[MnO_2]$ (mol dm^{-3})	10^4[cysteine] (mol dm^{-3})	$10^4[HClO_4]$ (mol dm^{-3})	Temp. (°C)	k_{obs} (s^{-1})
1.0	3.0	0.0	30	13.4
1.5				7.6
2.0				6.1
2.5				5.9
3.0				5.7
3.0	3.0	0.0	30	5.7
	4.0			7.6
	5.0			9.5
	6.0			11.5
	7.0			13.4
3.0	3.0	0.0	30	5.7
			40	7.6
			50	9.5
3.0	3.0	0.0	30	1.7
		0.93		5.3
		1.86		8.8
		2.79		11.2
		3.20		14.7
		3.72		17.2
		4.65		19.1
		5.58		19.2

colloidal MnO_2 by cysteine. The initial reaction of colloidal MnO_2 with cysteine or GSH indicate that the reaction is not first order with respect to colloidal $[(MnO_2)_n]$ (Tables 1 and 3). The decrease in the rate constant with $[MnO_2]$ is due to the possible coagulation of the colloidal particles. These observed results are in good agreement with the observations of Benito et al. [16, 18].

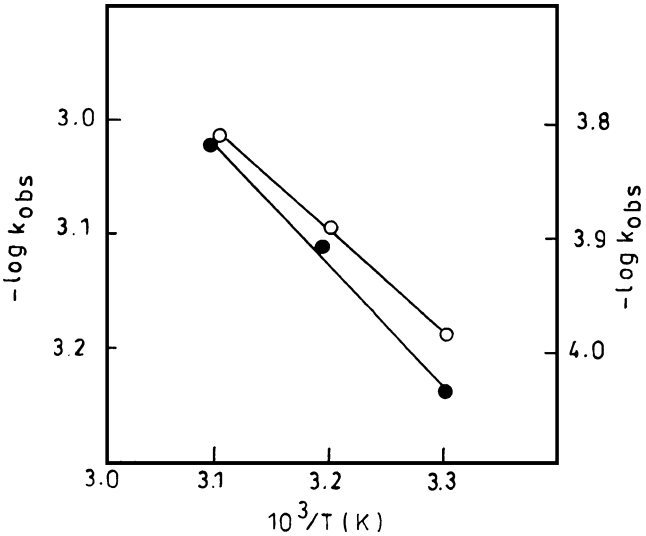

Fig. 5 Arrhenius plots for the oxidation of GSH [*open circles* (○)] and cysteine [*closed circles* (•)] by colloidal MnO_2. Reaction conditions: $[GSH]=8.0\times10^{-5}$ mol dm^{-3}; $[(MnO_2)_n]=8.0\times10^{-5}$ mol dm^{-3}; [cysteine]$=3.0\times10^{-4}$ mol dm^{-3}; $[(MnO_2)_n]=3.0\times10^{-5}$ mol dm^{-3}; temperature=30 °C

Activation parameters (E_a, $\Delta H^{\#}$ and $\Delta S^{\#}$) are believed to provide useful information regarding the environment in which the chemical reactions take place. Therefore, a series of kinetic runs were performed within the temperature range of 30 to 50 °C at constant MnO_2=(3.0×10^{-5} mol dm^{-3}) and cysteine=(3.0×10^{-4} mol dm^{-3}). The k_{obs} values (Table 2) were found to fit the Arrhenius Equation (Fig. 5). The nonlinear least square method was used to obtain the values of the parameters which are recorded in Table 2. The observations are consistent with the accepted view that a slow reaction would require higher energy of activation. On the other hand, the negative values of $\Delta S^{\#}$ indicate that the transition state is well structured and highly solvated. The following reactions are, therefore, considered to represent the most plausible mechanism of the reaction (Scheme 2).

In Schemes 1 and 2, reactions 1 and 10 represent, respectively, the adsorption of GSH and cysteine on the surface of colloidal MnO_2. After adsorption, the $(MnO_2)_n$–GSH and C2 undergo electron transfer process leading to the formation of radicals {reactions 2 and 11}. In the presence of $HClO_4$, the reaction proceeds through adsorption of H^+ on the surfaces of MnO_2 and GSH and forming C1 and C3, respectively. The rate-limiting step is a one step-one-electron transfer from reductant to colloidal MnO_2. Applying the steady-state approximation the rate law can be written as:

$$v = \frac{-d\left[(MnO_2)_n\right]}{dt} = \frac{\left(k_2K_{ad2} + k_2'K_{ad2}'K_p\left[H^+\right]^2\right)\left[(MnO_2)_n\right][cysteine]_T}{\left(1 + K_p\left[H^+\right]\right)} \quad (7)$$

Scheme 2 The reactions considered to represent the most plausible mechanism of the reaction

H^+ – independent

$$(MnO_2)_n + HSCH_2CH(NH_3^+)COO^- \overset{K_{ad2}}{\rightleftharpoons} (MnO_2)_n{-}HSCH_2CH(NH_3^+)COO^- \quad (10)$$

(C2)

$$C2 \xrightarrow{k_2} (MnO_2)_{n-1}{-}MnO_2H + \dot{S}CH_2CH(NH_3^+)COO^- \quad (11)$$

(radical)

H^+ – dependent

$$(MnO_2)_n + H^+ \overset{K_p}{\rightleftharpoons} (MnO_2)_n{-}H^+ \quad (12)$$

$$HSCH_2CH(NH_3^+)COO^- + H^+ \overset{K_a}{\rightleftharpoons} HSCH_2CH(NH_3^+)COOH \quad (13)$$

(A) **(HA)**

$$HA + (MnO_2)_n{-}H^+ \overset{K_{ad2}'}{\rightleftharpoons} H^+{-}(MnO_2)_n{-}HSCH_2CH(NH_3^+)COOH \quad (14)$$

(C3)

$$C3 \xrightarrow{k_2'} (MnO_2)_{n-1}{-}MnO_2H + Radical \quad (15)$$

$$(MnO_2)_{n-1}{-}MnO_2H + H^+ \xrightarrow{fast} Mn^{3+} + (MnO_2)_{n-1} + 2OH^- \quad (16)$$

$$Mn^{3+} + cysteine \xrightarrow{fast} Mn^{2+} + Radical \quad (17)$$

$$2\ Radicals \xrightarrow[dimerization]{fast} cystine\ (P) \quad (18)$$

and

$$k_{obs} = \frac{\left(k_2 K_{ad2} + k_2' K_{ad2}' K_p \left[H^+\right]^2\right)[cysteine]_T}{\left(1 + K_p\left[H^+\right]\right)} \quad (8)$$

Equation 8 is in agreement with the experimental results found for the reaction, as the orders in [cysteine] and [H^+] are first and fractional, respectively. In presence of [H^+], Eq. 8 can be reduced to Eq. 9.

$$k_{obs} = \frac{\left(k_2' K_{ad2}' \left[H^+\right]^2 [(MnO_2)_n][cysteine]_T\right)}{\left(1 + K_p\left[H^+\right]\right)} \quad (9)$$

We see that Eqs. 8 and 9 correspond to the two extreme conditions between which the reaction path depends on the [H^+].

To confirm the formation of Mn(III) as an intermediate, the effect of sodium fluoride was also studied under the same kinetic conditions. The presence of fluoride ions reduces the oxidation rate of GSH (Table 4) and cysteine (Fig. 6). A similar effect of fluoride ions was also observed previously [30, 31]. The inhibitory effect indicates the involvement of Mn(III) in the redox system. It has been established that Mn(II) acts as an autocatalyst in the permanganate oxidations of organic reductants [13–15, 34]. Therefore, the effect of externally added product, such as manganese(II), was also studied by varying [Mn(II)] from 2.0×10^{-4} to 40.0×10^{-4} mol dm^{-3} at constant colloidal [$(MnO_2)_n$], [reductant] and temperature. The rate constant increases with increase in Mn(II) (Table 4). The results are also shown in Fig. 6 for cysteine which indicates sigmoid dependence of k_{obs} on [Mn(II)].

Table 4 Effect of trapping agents (Mn(II) and F^-) on the oxidation of GSH (6.0×10^{-5} mol dm^{-3}) and cysteine (3.0×10^{-4} mol dm^{-3}) by colloidal MnO_2 at 30 °C

10^3[F^-] (mol dm^{-3})	k_{obs}[a] (mol^{-1} dm^3 s^{-1})	k_{obs}[b] (s^{-1})	10^4 [Mn (II)] (mol dm^{-3})	k_{obs}[a] (mol^{-1} dm^3 s^{-1})	$10^4 k_{obs}$[b] (s^{-1})
0.0	1.7	5.7	0.0	1.7	5.7
1.0	1.4	4.7	2.0	16.6	
2.0	1.3	4.2	4.0	12.4	
3.0	1.1	3.0	6.0	10.2	
4.0	1.0	1.9	8.0	9.0	
5.0	1.0	1.0	10.0	8.3	5.7
			15.0		7.6
			20.0		10.0
			30.0		12.2
			36.0		10.3
			40.0		7.6

[a] For GSH; colloidal [$(MnO_2)_n$]=8.0×10^{-5} mol dm^{-3}
[b] For cysteine; colloidal [$(MnO_2)_n$]=3.0×10^{-5} mol dm^{-3}

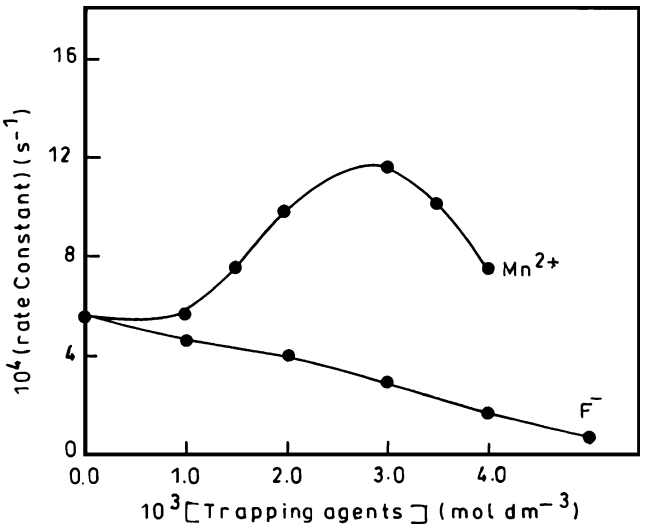

Fig. 6 Effect of trapping agents on the rate constant for the oxidation of cysteine. Reaction conditions: [cysteine]=3.0×10^{-4} mol dm^{-3}; [$(MnO_2)_n$]=3.0×10^{-5} mol dm^{-3}; temperature=30 °C

Our results seem to suggest that Mn(II) is the active autocatalyst (the Mn(II) formed as the reaction product contributes to accelerate the oxidations of GSH and cysteine by colloidal MnO_2).The reduction of colloidal MnO_2 by Mn(II) has already been postulated [35]. To decide the role of Mn(II), some kinetic experiments were also performed for the reduction of colloidal MnO_2 by Mn (II) in the absence of GSH or cysteine. For colloidal MnO_2=8.0×10^{-5} mol dm^{-3} and temperature=30 °C, the values of $k_{obs}(10^{-4})$ were found to be 0.7, 1.5, 1.0, 1.5, 1.5 s^{-1} for [Mn(II)]=2.0, 3.0, 6.0, 10.0 and 20.0×10^{-5} mol dm^{-3}, respectively. It was observed that the reactivity of Mn(II) is ca. tenfold slower than S-containing reductant, i.e., cysteine. The probability of a direct reaction between colloidal MnO_2 and Mn(II) to yield Mn(III) without the participation of GSH or cysteine cannot be ruled out or might be of minor significance. In the presence of Mn(II), there is a competition between GSH or cysteine and Mn(II)

Table 5 Values of second-order rate constants (k^{II}) for the reaction of colloidal MnO_2 with different reductants in aqueous neutral medium at 30 °C

Reductants	10^2 k^{II}(mol^{-1} dm^3 s^{-1})	Reference
Glutathione[a]	230	Present work
Thiourea[b]	18	27
Cysteine[c]	191	Present work
Glycine[c]	No reaction	Present work
Glutamic acid[c]	No reaction	Present work

[a] [$(MnO_2)_n$]=8.0×10^{-5} mol dm^{-3}, [GSH]=8.0×10^{-5} mol dm^{-3}
[b] [$(MnO_2)_n$]=5.0×10^{-5} mol dm^{-3}, [thiourea]=6.0×10^{-4} mol dm^{-3}
[c] [$(MnO_2)_n$]=3.0×10^{-5} mol dm^{-3}, [cysteine]=6.0×10^{-4} mol dm^{-3}, [glycine]=6.0×10^{-4} mol dm^{-3}, [glutamic acid]=6.0×10^{-4} mol dm^{-3}

to react with the colloidal MnO_2. Therefore, the exact dependence of rate constants on Mn(II) cannot be predicted.

Oxidation of glutamic acid and glycine

To see whether or not the –COOH and $–NH_2$ groups of GSH and cysteine are equally responsible for the oxidation of GSH and cysteine, the oxidation of glutamic acid and glycine (structural units of GSH) was also investigated under similar experimental conditions, i.e., [oxidant]= 1.0×10^{-5} to 3.0×10^{-5} mol dm^{-3}, [reductant]=3.0×10^{-4} to 7.0×10^{-4} mol dm^{-3}, temperature=30 °C. No decay in the absorbance of colloidal MnO_2 was noticed under any of these conditions. These results are interesting but not surprising because the reactivity of S-bonded reductants is higher in comparison to N- and O-bonded. These observations undoubtedly show that the –SH group of GSH and cysteine, respectively, is responsible for the reduction of colloidal MnO_2.

Reactivity of colloidal MnO_2

Table 5 summarizes the values of the second-order rate constant (k^{II}, mol^{-1} dm^3 s^{-1}) for the reactivity of –SH containing reductants and structural units of GSH towards colloidal MnO_2. Based on their reactivity, the reductants can be ordered as GSH>cysteine>thiourea. Interestingly, the reactivity of thiourea toward colloidal MnO_2 is much lower than the corresponding oxidation of GSH and cysteine under the same experimental conditions. The reactivity of –SH group depends on the experimental conditions. Under our experimental conditions, [reductant]= 8.0×10^{-5} to 6.0×10^{-4} mol dm^{-3}, [oxidant]=3.0×10^{-5} to 8.0×10^{-5} mol dm^{-3}, temperature=30 °C, only the –SH group is responsible for the oxidation of GSH and cysteine. The presence of C=S in thiourea appears to inhibit, but not totally prevent, the electron transfer to colloidal MnO_2. It has been established on several occasions [24, 36] that the OH group of the substrate is responsible for the adsorption of the reactant on the surface of colloidal MnO_2 through hydrogen bonding. Though the data are not conclusive, it seems that the higher reactivity of GSH in comparison to cysteine may be due to the presence of a higher number of OH groups in GSH.

References

1. McAuley A, Olatunji MA (1977) Can J Chem 55:3328
2. Connett PH, Wetterhahn KE (1985) J Am Chem Soc 107:4282
3. Connett PH, Wetterhahn KE (1986) J Am Chem Soc 108:1842
4. Perez-Benito JF, Arias C, Lamrhari D (1994) New J Chem 18:663
5. Herszage J, Afonso MDS, Luther III G (2003) Environ Sci Technol 37:3332
6. McAuley A, McCann JP (1975) J Chem Soc Dalton 783
7. Olatunji MA, McAuley A (1977) Can J Chem 55:3335
8. Olatunji MA, Ayoko GA (1988) Polyhedron 7:11
9. Wiberg KB, Deutsch CJ, Rocek J (1973)J Am Chem Soc 95:3034
10. Simándi LI, Jáky M (1976) J Am Chem Soc 98:1995
11. Simándi LI, Jáky M, Freeman F, Fuselier CO, Karchefski EM (1978) Inorg Chim Acta 31:L457
12. Freeman F, Fuselier CO, Armstead CR, Dalton CE, Davidson PA, Karchefski EM, Krochman DE, Johnson MN, Jones NK (1981) J Am Chem Soc 103:1154
13. Freeman F, Kappos JC (1985) J Am Chem Soc 107:6628
14. Freeman F, Kappos JC (1989) J Org Chem 54:2730
15. Mata-Perez F, Perez-Benito JF (1987) Can J Chem 65:2373
16. Perez-Benito JF, Arias C, Brillas E (1990) Int J Chem Kinet 22:261
17. Perez-Benito JF, Lee DG (1985) Can J Chem 63:3545
18. Perez Benito JF, Arias C (1992) J Colloid Interface Sci 149:92
19. Perez-Benito JF, Lee DG (1985) Can J Chem 63:1275
20. Perez Benito JF, Arias C (1991) Int J Chem Kinet 23:717
21. Perez Benito JF, Arias C, Amat EJ (1996) J Colloid Interface Sci 177:288
22. Khan Z, Raju, Akram M, Kabir-ud-Din (2004) Int J Chem Kinet 36:356
23. Kabir-ud-Din, Iqubal SMS, Khan Z (2005) Colloid Polym Sci 283:504
24. Kabir-ud-Din, Iqubal SMS, Khan Z (2005) Inorg React Mech 5:151
25. Khan Z, Kumar P, Kabir-ud-Din (2004) Colloids Surf A Physicochem Eng Asp 248:25
26. Kumar P, Khan Z (2005) Carbohydr Res 340:1365
27. Andrabi SMZ, Khan Z (2005) Colloid Polym Sci 284:36
28. Bastian EJ Jr, Martin RB (1973) J Phys Chem 77:1129
29. Olatunji MA, McAuley A (1975) J Chem Soc Dalton 682
30. Kwong DW, Pennington DE (1984) Inorg Chem 23:2528
31. Ghosh SK, Gould ES (1989) Inorg Chem 28:3651
32. Abedinzadeh Z, Gardes M-Albert, Ferradins C, (1989) Can J Chem 67:1247
33. Lin CT, Beattie JK (1972) J Am Chem Soc 94:3011
34. Girgis MM, El-Shatoury SA, Khalil ZH (1985) Can J Chem 63:3317
35. Perez Benito JF (2002) J Colloid Interface Sci 248:130
36. Tuncay M, Yuce N, Arlkan B, Gokturk S, (1999) Colloids Surf A 149:79